J Solid State Electrochem (2012) 16:2011–2016
DOI 10.1007/s10008-011-1611-5

ORIGINAL PAPER

Synthesis and electrochemical properties of spinel $Li_4Ti_5O_{12-x}Cl_x$ anode materials for lithium-ion batteries

Yudai Huang · Yanling Qi · Dianzeng Jia · Xingchao Wang · Zaiping Guo · Won Il Cho

Received: 13 August 2011 / Revised: 27 November 2011 / Accepted: 30 November 2011 / Published online: 13 December 2011
© Springer-Verlag 2011

Abstract $Li_4Ti_5O_{12-x}Cl_x$ ($0 \le x \le 0.3$) compounds were synthesized successfully via high temperature solid-state reaction. X-ray diffraction and scanning electron microscopy were used to characterize their structure and morphology. Cyclic voltammetry, electrochemical impedance spectroscopy, and charge/discharge cycling performance tests were used to characterize their electrochemical properties. The results showed that the $Li_4Ti_5O_{12-x}Cl_x$ ($0 \le x \le 0.3$) compounds were well-crystallized pure spinel phase and that the grain sizes of the samples were about 3–8 μm. The $Li_4Ti_5O_{11.8}Cl_{0.2}$ sample presented the best discharge capacity among all the samples and showed better reversibility and higher cyclic stability compared with pristine $Li_4Ti_5O_{12}$. When the discharge rate was 0.5 C, the $Li_4Ti_5O_{11.8}Cl_{0.2}$ sample presented the superior discharge capacity of 148.7 mAh g^{-1}, while that of the pristine $Li_4Ti_5O_{12}$ was 129.8 mAh g^{-1}; when the discharge rate was 2 C, the $Li_4Ti_5O_{11.8}Cl_{0.2}$ sample presented the discharge capacity of 120.7 mAh g^{-1}, while that of the pristine $Li_4Ti_5O_{12}$ was only 89.8 mAh g^{-1}.

Keywords $Li_4Ti_5O_{12-x}Cl_x$ · Anode materials · Solid-state reaction · Lithium-ion batteries

Introduction

Spinel $Li_4Ti_5O_{12}$ [1] is a promising anode material for lithium-ion batteries. The excellent cycling performance and long life of spinel $Li_4Ti_5O_{12}$ make it a good candidate as an anode electrode, especially for larger scale applications. Its potential is ascribed to its unique characteristics, such as good structural stability with almost negligible volume change in the charge/discharge process, so it is regarded as a "zero strain" insertion material [2], which may enable $Li_4Ti_5O_{12}$ electrode to have excellent Li^+ insertion and extraction reversibility. Moreover, it offers a discharge platform around 1.55 V versus Li^+/Li, above the reduction potential of most organic electrolytes. Consequently, passive films with high resistances from the reduction of electrolytes at the solid electrolyte interphase can be avoided on the $Li_4Ti_5O_{12}$ surface [3]. This voltage is also sufficiently high for avoiding the formation of metallic lithium. However, $Li_4Ti_5O_{12}$ exhibits poor electronic and lithium-ionic conductivities [4, 5], thereby limiting its rate capability. Intensive research has particularly focused on improving the rate capacity and has suggested numerous solutions.

Y. Huang · Y. Qi · D. Jia · X. Wang
Key Laboratory of Clean Energy Material and Technology of the Ministry of Education, Xinjiang University, Urumqi, People's Republic of China

Y. Huang · Y. Qi · D. Jia · X. Wang
Key Laboratory of Advanced Functional Materials of the Autonomous Region, Xinjiang University, Urumqi, People's Republic of China

Y. Huang · Y. Qi · D. Jia (✉) · X. Wang
Institute of Applied Chemistry, Xinjiang University, Urumqi 830046 Xinjiang, People's Republic of China
e-mail: jdz0991@gmail.com

Z. Guo
Institute for Superconducting and Electronic Materials, University of Wollongong, Wollongong, NSW 2522, Australia

W. I. Cho
Energy Storage Research Center, Korea Institute of Science and Technology, 39-1, Hawolgok-dong, Seongbuk-gu, Seoul 136-791, Republic of Korea

Among these projects, the doping strategy [6–8] is considered to be an effective path to improve the electrochemical performance of spinel $Li_4Ti_5O_{12}$. Following this trend, there are a large number of reports on doping various metal cations (V^{5+}, Mn^{4+}, Fe^{3+}, etc.) into Li or Ti sites [9–12]. However, very few studies have been focused on improving the anode electrode rate capacity at high current density through doping non-metal anions into O sites until now. In 2009, Qi et al. [13] reported that the introduction of Br into the spinel structure could improve the rate capacity of $Li_4Ti_5O_{12}$. The interesting results derived from the anion doping stimulated our research interest in investigating the effects of other types of anion doping. To the best of our knowledge, up to now, no Cl-doped anode materials ($Li_4Ti_5O_{12-x}Cl_x$) have been reported. In this study, cubic spinel structure $Li_4Ti_5O_{12-x}Cl_x$ ($0 \le x \le 0.3$) compounds with excellent characteristics were synthesized successfully for the first time by means of conventional solid-state reaction. The structures, morphologies, and electrochemical properties of these materials were also investigated.

Experimental

$Li_4Ti_5O_{12-x}Cl_x$ (x=0, 0.1, 0.2, and 0.3) compounds were prepared by conventional high temperature solid-state reaction using $LiOH{\cdot}H_2O$ (A.R., Tianjinshixin, China), $LiCl{\cdot}H_2O$ (A.R., Xi'anhuaxue, China), and anatase-type TiO_2 (A.R., Tianjinfuchen, China) in a Li/Ti molar ratio of 4.35:5. Excess Li was provided to compensate for its loss during the high temperature synthesis [4]. The reagents were mixed by the dry method in an agate mortar and ground with a pestle for 1 h to prepare the four precursor powders of $Li_4Ti_5O_{12-x}Cl_x$ (x=0, 0.1, 0.2, and 0.3). The mixed reactant mixtures were heated in a muffle furnace at 800 °C for 12 h in air, followed by natural cooling to room temperature. The synthesized samples were reground before powder characterization and electrode preparation. The stoichiometry of Li and Ti in the as-prepared samples was confirmed by the inductively coupled plasma technique. The results showed that the true molar ratio of Li to Ti was 4.17:5 in the samples.

The thermal decomposition behavior of the mixed precursors was examined by thermogravimetric analysis (TGA) and differential thermal analysis (DTA) (TGA-DTA, STA449C, NETZSCH, Germany) at a heating rate of 10 °Cmin^{-1}. Powder X-ray diffraction (XRD, MXP18AHF, MAC, Japan) using CuKα radiation (λ=1.54056 Å) was used to identify the phase composition and crystal lattice parameters of the synthesized powders. The surface morphology of the samples was observed using a scanning electron microscopy (SEM JEOL, JSM-6460A, Japan). $Li_4Ti_5O_{12-x}Cl_x$ powders were thoroughly mixed with 5% polyvinylidene fluoride and 10% acetylene black in *N*-methylpyrrolidone. The obtained slurries were then brushed onto a copper foil substrate and dried in a vacuum oven at 120 °C for 8 h, respectively. Lithium foil was used as the counter electrode, and Celgard 2400 microporous polyethylene membrane as the separator. The electrolyte was a mixture of 1 M $LiPF_6$ in ethylene carbonate/diethyl carbonate (1:1 by volume). The cells were assembled in an argon-filled glove box and were left to age for at least 12 h before charge and discharge testing at different current densities. The charge/discharge cycling was performed on a battery test instrument (CT2001A, LAND Battery Program-control Test System, China) over a voltage range of 1.0–3.0 V at room temperature. Cyclic voltammetry (CV) was carried out on a CHI600B electrochemical workstation (CHI, 600B, CHENHUA, China) in the potential range of 1.0–3.0 V at a scan rate of 0.1 mV s^{-1}. Electrochemical impedance spectroscopy (EIS) measurements were performed using an impedance system (IM6ex, Zahner Elektrik, Germany). The spectra were potentiostatically measured by applying an ac voltage of 5 mV over the frequency range from 0.01 Hz to 100 kHz.

Results and discussion

The TGA and DTA results of the mixed precursors of $Li_4Ti_5O_{12-x}Cl_x$ are similar, so the TGA and DTA results of the mixed precursors of $Li_4Ti_5O_{11.8}Cl_{0.2}$ are shown as an example in Fig. 1. The loss of weight in the temperature range between 130 and 200 °C is due to the loss of crystal water in the mixed precursors, which corresponds to an endothermic peak on the DTA curve at 135 °C. The loss of weight in the temperature range between 200 and 780 °C is associated with the decomposition and combustion of the constituents in the mixed precursors and also due to the transformation of lithium titanium oxide, which corresponds to an exothermic peak on the DTA curve at about 460 °C.

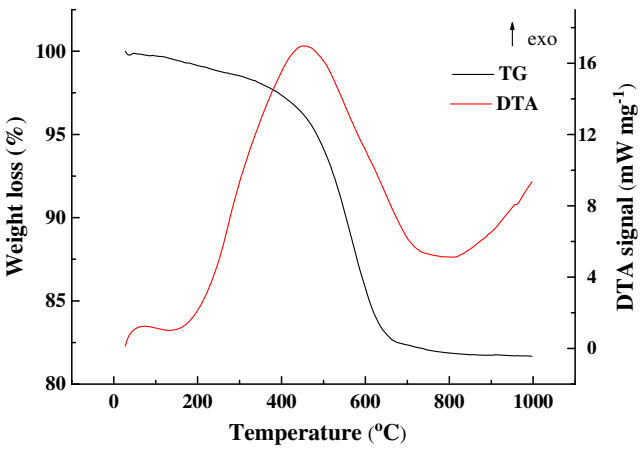

Fig. 1 TGA-DTA curves of the precursor for $Li_4Ti_5O_{11.8}Cl_{0.2}$

After 780 °C, virtually no loss of weight is found. $Li_4Ti_5O_{11.8}Cl_{0.2}$ could be obtained by annealing at temperatures higher than 780 °C, so the annealing temperature was chosen to be 800 °C.

The XRD patterns of the synthesized lithium titanate oxide samples with and without Cl doping are shown in Fig. 2. The diffraction peaks of $Li_4Ti_5O_{12-x}Cl_x$ (x=0, 0.1, 0.2, and 0.3) can be indexed as cubic spinel $Li_4Ti_5O_{12}$. The pure spinel $Li_4Ti_5O_{12}$ samples were also synthesized successfully by means of solid-state reaction, and there are no other impurity peaks. Doping with Cl does not change the structure of cubic spinel $Li_4Ti_5O_{12}$, indicating that the synthesized samples are in accordance with the spinel $Li_4Ti_5O_{12}$ standard in the Joint Committee on Powder Diffraction Standards database (JCPDS no. 49-0207), so that the dopant Cl has clearly entered the lattice structure of $Li_4Ti_5O_{12}$ without causing any changes in its structural characteristics [13]. The XRD fitting results, which are shown in Table 1, indicate that the cubic lattice parameter increases with increasing Cl doping (from 0 to 0.3). The lattice parameter linearly increases from 8.3973 Å for the undoped $Li_4Ti_5O_{12}$ to 8.4203 Å for $Li_4Ti_5O_{11.9}Cl_{0.1}$, 8.4441 Å for $Li_4Ti_5O_{11.8}Cl_{0.2}$, and 8.4632 Å for $Li_4Ti_5O_{11.7}Cl_{0.3}$. The products doped with Cl ion have larger lattice parameter, which is ascribed to the Cl ion substitution for O ion. The ionic radius of the Cl ion (1.7 Å) is larger than that of the O ion (1.4 Å), and Cl ion substitution will lead to the reduction of part of the Ti^{4+} ion to larger Ti^{3+} ion as charge compensation, which results in the increase in the samples' lattice parameter. The trend in the morphology variation for different $Li_4Ti_5O_{12-x}Cl_x$ compounds is similar, so SEM images of $Li_4Ti_5O_{12}$ and $Li_4Ti_5O_{11.8}Cl_{0.2}$ are presented as examples in Fig. 3. SEM observations of the investigated samples indicated that Cl-doping did not obviously change the particle size of pure $Li_4Ti_5O_{12}$,

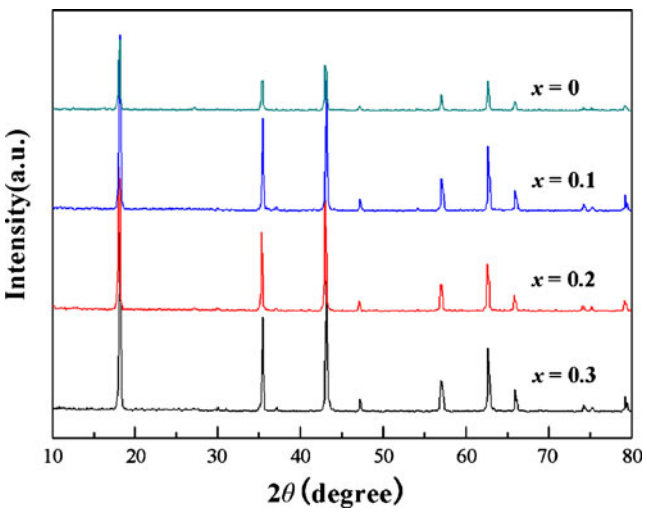

Fig. 2 XRD patterns of $Li_4Ti_5O_{12-x}Cl_x$ (x=0, 0.1, 0.2, and 0.3)

Table 1 Variation in crystal lattice parameter for $Li_4Ti_5O_{12-x}Cl_x$ (x=0, 0.1, 0.2, and 0.3)

Sample	Lattice parameter (Å)	Errors (Å)
$Li_4Ti_5O_{12}$	8.3973	0.0027
$Li_4Ti_5O_{11.9}Cl_{0.1}$	8.4203	0.0035
$Li_4Ti_5O_{11.8}Cl_{0.2}$	8.4441	0.0048
$Li_4Ti_5O_{11.7}Cl_{0.3}$	8.4632	0.0028

but agglomeration between particles was observed to a certain extent in the undoped sample. All the samples are in particle form, and the particle size is 3–8 μm.

Figure 4 displays discharge capacity versus cycle number curves for $Li_4Ti_5O_{12-x}Cl_x$ (x=0, 0.1, 0.2, and 0.3) between 1.0 and 3.0 V at 0.5 C at room temperature. From Fig. 4, we can see that the capacity of $Li_4Ti_5O_{12-x}Cl_x$ (x=0, 0.1, 0.2) increases with increasing Cl doping. The $Li_4Ti_5O_{11.9}Cl_{0.1}$ and $Li_4Ti_5O_{11.8}Cl_{0.2}$ samples have larger discharge capacity than the pure $Li_4Ti_5O_{12}$ spinel. At the low discharge rate of 0.5 C, the $Li_4Ti_5O_{11.8}Cl_{0.2}$ sample presents the best discharge capacity of 148.7 mAh g^{-1} (at the second cycle) among all the samples, while the discharge capacity of the pure $Li_4Ti_5O_{12}$ is much lower (129.8 mAh g^{-1} at the third cycle). The initial capacities of the samples are relatively low because the electrode materials are not completely invoked during the initial charge/discharge process. The improvement in capacity for the doped samples could be attributed to the Cl ion doped into the lattice of $Li_4Ti_5O_{12}$. The mode of action may be that the paths for insertion and extraction of Li^+ become broader as the lattice parameter increases, as shown in Table 1, and insertion and extraction of Li^+ become easier compared with the pristine $Li_4Ti_5O_{12}$ [14]. In the $Li_4Ti_5O_{12}$ structure, 75% of Li^+ are located at tetrahedral 8 *a* sites, while 25% of the Li^+ and the Ti^{4+} are randomly distributed at octahedral 16*d* sites, while O^{2-} occupy the 32 *e* sites, and the 8 *b*, 48 *f*, and 16 *c* sites are empty. During the lithiation process, 3 Li^+ can be accommodated by one $Li_4Ti_5O_{12}$ formula unit, which will make spinel $Li_4Ti_5O_{12}$ transform to rock-salt $Li_7Ti_5O_{12}$. $Li_7Ti_5O_{12}$ is a good electronic conductor because the average oxidation state of Ti is +3.4 in this lithiated phase, meaning that there is coexistence of Ti^{3+} (60%) and Ti^{4+} (40%) ions in the lattice [15]. Cl^- partially substitute for O^{2-}, which will increase the quantities of Ti^{3+} needed to compensate for the deficit of negative charges caused by Cl-doping into $Li_7Ti_5O_{12}$, which will improve the ionic conductivity of $Li_7Ti_5O_{12}$. In addition, we can see clearly from Fig. 4 that the discharge capacity of the $Li_4Ti_5O_{11.7}Cl_{0.3}$ sample is obviously decreased compared with the $Li_4Ti_5O_{11.8}Cl_{0.2}$ sample, even lower than that of the pure $Li_4Ti_5O_{12}$. The results indicate that the Cl-doping in $Li_4Ti_5O_{12}$ has an optimal value. In this work, the optimum amount of Cl-doping

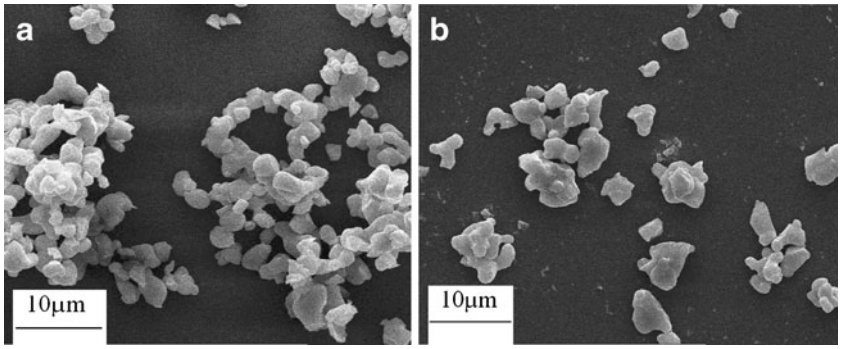

Fig. 3 SEM images of the $Li_4Ti_5O_{12}$ and $Li_4Ti_5O_{11.8}Cl_{0.2}$ samples: **a** $Li_4Ti_5O_{12}$; **b** $Li_4Ti_5O_{11.8}Cl_{0.2}$

is x=0.2. Therefore, $Li_4Ti_5O_{11.8}Cl_{0.2}$ exhibits a relatively high specific capacity and excellent cycling stability.

To compare the differences in the electrochemical properties between the $Li_4Ti_5O_{12}$ and $Li_4Ti_5O_{11.8}Cl_{0.2}$ samples, EIS of the two samples was conducted before cycling. Figure 5 shows the electrochemical impedance spectra of $Li_4Ti_5O_{12}$ and $Li_4Ti_5O_{11.8}Cl_{0.2}$. The plots are similar to each other in shape, with a semicircle appearing in the high frequency domain and a straight line in the low frequency region. The depressed semicircle in the moderate frequency region is attributed to the charge transfer process [16, 17]. By comparing the results, it can be seen that the semicircle for the $Li_4Ti_5O_{11.8}Cl_{0.2}$ sample is smaller than that of the $Li_4Ti_5O_{12}$ sample. The charge transfer resistance of the $Li_4Ti_5O_{11.8}Cl_{0.2}$ electrode is around 50 Ω cm^{-2}, while that of $Li_4Ti_5O_{12}$ electrode is above 140 Ω cm^{-2}. This indicates that the $Li_4Ti_5O_{11.8}Cl_{0.2}$ sample has decreased charge transfer resistance, which is not unexpected, as Cl^- substitution for O^{2-} in $Li_4Ti_5O_{12}$ will cause the generation of mixing valence of Ti^{3+}/Ti^{4+} as charge compensation, thereby enhance the electronic conductivity of $Li_4Ti_5O_{12}$ [4], which is in good agreement with the electrochemical results of Fig. 4.

Cyclic voltammograms (CV curves) of the $Li_4Ti_5O_{12}$ and $Li_4Ti_5O_{11.8}Cl_{0.2}$ samples are shown in Fig. 6. The curves of the two samples are almost the same, and they show one cathodic peak located at 1.50 V, corresponding to the voltage plateau of the first discharge process [16]. This represents the process of Li^+ insertion into spinel $Li_4Ti_5O_{12}$. They also show an anodic peak at 1.68 V (vs. Li), which corresponds to the voltage plateau of the first charge process, representing the Li^+ extraction from the spinel $Li_4Ti_5O_{12}$. This is a typical behavior for a two-phase reaction during Li^+ extraction and insertion process [18]. It is obvious that the pair of reversible redox peaks of the $Li_4Ti_5O_{11.8}Cl_{0.2}$ sample are enlarged and sharpened compared with those of the pure $Li_4Ti_5O_{12}$. This indicates that the dopant Cl does not change the electrochemical reaction process of $Li_4Ti_5O_{12}$ in this voltage range but boosts the charge/discharge specific capacity of $Li_4Ti_5O_{12}$, which is consistent with the discharge curves of Fig. 4.

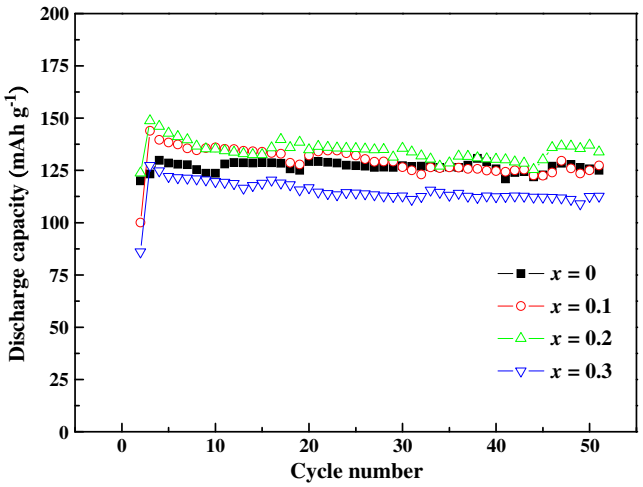

Fig. 4 Discharge capacity vs. cycle number curves of $Li_4Ti_5O_{12-x}Cl_x$ (x=0, 0.1, 0.2, and 0.3) at 0.5 C

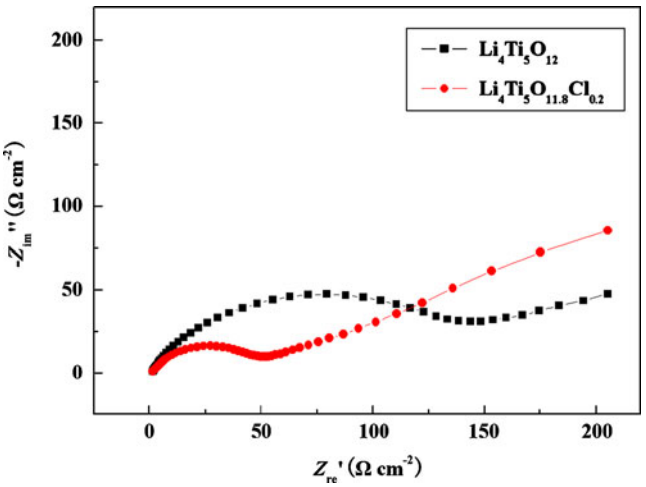

Fig. 5 Electrochemical impedance spectra of $Li_4Ti_5O_{12}$ and $Li_4Ti_5O_{11.8}Cl_{0.2}$

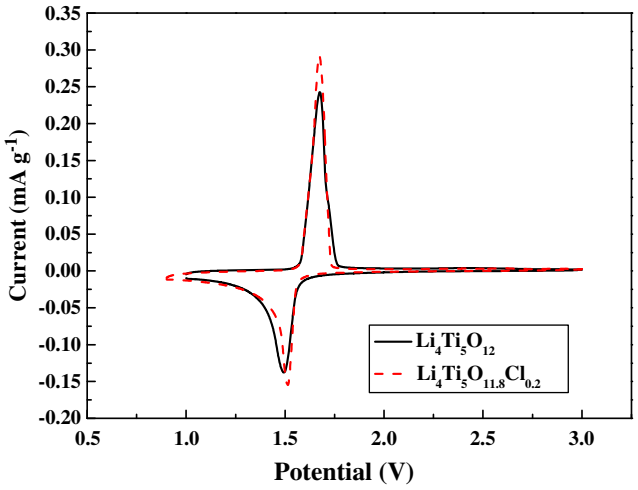

Fig. 6 Cyclic voltammograms of $Li_4Ti_5O_{11.9}Cl_{0.2}$ and pristine $Li_4Ti_5O_{12}$

Discharge tests at different current densities illustrate more interesting results. Figure 7 shows the cycling performances of $Li_4Ti_5O_{12}$ and $Li_4Ti_5O_{11.8}Cl_{0.2}$ electrodes as a function of cycle number at different current densities (1 and 2 C), respectively. As can be observed in Fig. 7, the initial capacities of the two samples, whether at 1 or 2 C, are relatively low because the electrode materials are not completely invoked during the initial charge/discharge process. After the initial capacity, the $Li_4Ti_5O_{11.8}Cl_{0.2}$ sample shows higher discharge capacity and better capacity retention with further cycling than the $Li_4Ti_5O_{12}$ sample. With increasing current density, the samples still maintain excellent cycling performance. However, the discharge capacity is slightly higher at 1 C than at 2 C for both $Li_4Ti_5O_{11.8}Cl_{0.2}$ and $Li_4Ti_5O_{12}$. For the $Li_4Ti_5O_{11.8}Cl_{0.2}$ sample, the highest discharge capacities are 133.3 and 120.3 mAh g^{-1}, and the discharge capacities are 122.5 and 102.2 mAh g^{-1} after 50 cycles at 1 and 2 C, respectively. For the $Li_4Ti_5O_{12}$ sample, the highest discharge capacities are 110.9 and 87.3 mAh g^{-1}, and the discharge capacities are 108.2 and 76.5 mAh g^{-1} after 50 cycles at 1 and 2 C, respectively. These results obtained from Fig. 7 make it clear that doping with Cl can improve the capacity and cyclic reversibility of $Li_4Ti_5O_{12}$.

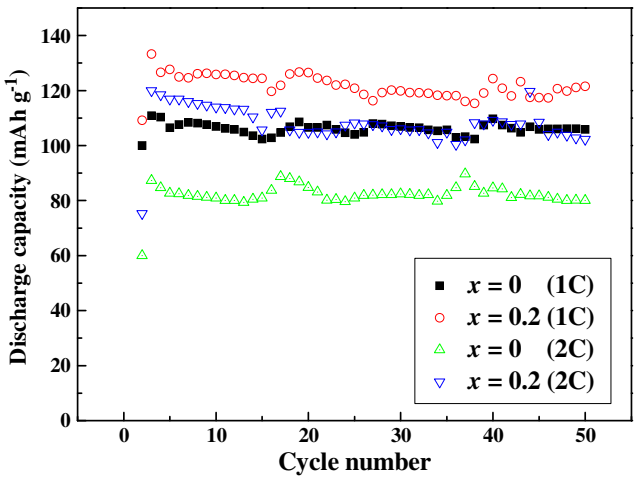

Fig. 7 Discharge curves of $Li_4Ti_5O_{12-x}Cl_x$ (x=0, 0.2) at 1 and 2 C, respectively

Although the electrochemical properties of $Li_4Ti_5O_{11.8}Cl_{0.2}$ are better than those of $Li_4Ti_5O_{12}$, the capacity was not high for any of these $Li_4Ti_5O_{12-x}Cl_x$ ($0 \le x \le 0.3$) materials, which may be ascribed to the following factors: Firstly, the ratio of Li to Ti in the materials is 4.17:5, not 4:5. During the intercalation of Li^+ into the $Li_4Ti_5O_{12}$ structure, Li^+ begin to occupy 16 *c* sites. Then, Li^+ in the tetrahedral 8 *a* sites also migrate to 16 *c* sites. Eventually, all 16 *c* sites are occupied by Li^+. Accordingly, the overall insertion capacity of $Li_4Ti_5O_{12}$ is limited by the number of free octahedral sites that can accommodate Li^+. When the spinel host structure is in accordance with $[Li]_{8a}[Li_{1/3}Ti_{5/3}]_{16d}[O_4]_{32e}$, it can accommodate maximum Li^+ content without significant change in the lattice constant. Consequently, this material shows good capacity. If there are excessive Li^+ in the raw material, a small amount of Li^+ may be intercalated into the spinel $Li_4Ti_5O_{12}$ lattice during the heat treatment, thus reducing the amount of intercalated Li^+ in the subsequent electrochemical reaction. This may somewhat decrease the capacity of the $Li_4Ti_5O_{12}$ material [18]. Secondly, in the high temperature solid-state reaction, the morphology of $Li_4Ti_5O_{12}$ is very difficult to control, so the morphology of $Li_4Ti_5O_{12}$ is anomalous, and the particle size is bigger than that obtained by liquid methods. It is very difficult for the electrolyte to penetrate the lithium titanate oxide electrode, thus affecting the electrochemical properties of the $Li_4Ti_5O_{12}$. Thirdly, the dry method using a mortar and pestle was selected to mix the precursors, which could not confer complete mixing of the Li- and Ti-precursors.

Conclusions

Cubic spinel $Li_4Ti_5O_{12-x}Cl_x$ ($0 \le x \le 0.3$) samples were synthesized successfully by conventional high-temperature solid-state reaction. Cl-doping increases the specific capacity significantly. The substitution of Cl^- into O^{2-} sites can increase the amount of Ti^{3+}/Ti^{4+} mixing as charge compensation and thus not only decreases the charge transfer resistance of $Li_4Ti_5O_{12-x}Cl_x$ ($0 \le x \le 0.3$), but also improves the lithium-ion diffusion. Both aspects have a strong impact on the electrochemical properties of $Li_4Ti_5O_{12}$ electrode. However, there is an optimum amount of Cl-doping. From the overall performance point of view, the $Li_4Ti_5O_{11.8}Cl_{0.2}$ sample shows the best discharge capacity under these experimental conditions. The as-prepared $Li_4Ti_5O_{11.8}Cl_{0.2}$ product exhibits capacity as high as 148.7 mAh g^{-1} at 0.5 C and

maintains around 133.8 mAh g^{-1} after 50 cycles, which makes $Li_4Ti_5O_{11.8}Cl_{0.2}$ a promising anode material for lithium-ion batteries.

Acknowledgments This work was supported by the Natural Science Foundation of Xinjiang Province (no. 200821121), the National Natural Science Foundation of China (no. 21161021), the Technological People Service Corporation (no. 2009GJG40028), the Science and Technology Foundation of Urumqi (nos. y08231006 and ZD8113007), the Science and Technology Foundation of Xinjiang University (no. BS100114), and the Program for Changjiang Scholars and Innovative Research Team in University of Ministry of Education of China (no. IRT1081).

References

1. Yuan T, Cai R, Gu P, Shao Z (2010) J Power Sources 195:2883–2887
2. Hao Y-J, Lai Q-Y, Chen Y-D, Lu J-Z, Ji X-Y (2008) J Alloys Compd 462:404–409
3. Prosini PP, Mancini R, Petrucci L, Contini V, Villano P (2001) Solid State Ionics 144:185–192
4. Zhao H, Li Y, Zhu Z, Lin J, Tian Z, Wang R (2008) Electrochim Acta 53:7079–7083
5. Huang S, Wen Z, Zhang J, Gu Z, Xu X (2006) Solid State Ionics 177:851–855
6. Hao Y-J, Lai Q-Y, Lu J-Z, Ji X-Y (2007) Ionics 13:369–373
7. Zhong Z (2007) Electrochem Solid State Lett 10:A267–A269
8. Chen CH, Vaughey JT, Jansen AN, Dees DW, Kahaian AJ, Goacher T, Thackeray MM (2001) J Electrochem Soc 148: A102–A104
9. Huang S, Wen Z, Zhu X, Lin Z (2007) J Power Sources 165:408–412
10. Kubiak P, Garcia A, Womes M, Aldon L, Olivier-Fourcade J, Lippens P-E, Jumas J-C (2003) J Power Sources 119–121:626–630
11. Mukai K, Ariyoshi K, Ohzuku T (2005) J Power Sources 146:213–216
12. Park HE, Seong IW, Yoon WY (2009) J Power Sources 189:499–502
13. Qi Y, Huang Y, Jia D, Bao S-J, Guo ZP (2009) Electrochim Acta 54:4772–4776
14. Huang Y, Jiang R, Bao S-J, Dong Z, Cao Y, Jia D, Guo Z (2009) J Solid State Electrochem 13:799–805
15. Yao XL, Xie S, Nian HQ, Chen CH (2008) J Alloys Compd 465:375–379
16. Guo ZP, Zhong S, Wang GX, Liu HK, Dou SX (2003) J Alloys Compd 348:231–235
17. Robertson AD, Trevino L, Tukamoto H, Irvine JTS (1999) J Power Sources 81–82:352–460
18. Hao Y, Lai Q, Liu D, Xu Z, Ji X (2005) Mater Chem Phys 94:382–387